Cardiovascular Research (2010) **87**, 524–534
doi:10.1093/cvr/cvq068

Influence of p53 in the transition of myotrophin-induced cardiac hypertrophy to heart failure

Biswajit Das[1], David Young[1], Amit Vasanji[2], Sudhiranjan Gupta[1†], Sagartirtha Sarkar[1‡], and Subha Sen[1*]

[1]Department of Molecular Cardiology-NB50, Lerner Research Institute, Cleveland Clinic, 9500 Euclid Avenue, Cleveland, OH 44195, USA; and [2]Biomedical Imaging and Analysis Core, Lerner Research Institute, Cleveland Clinic, 9500 Euclid Avenue, Cleveland, OH 44195, USA

Received 14 October 2009; revised 27 January 2010; accepted 23 February 2010; online publish-ahead-of-print 3 March 2010

Time for primary review: 39 days

Aims Cardiac-specific overexpression of myotrophin (myo) protein in transgenic (myo-Tg) mice results in hypertrophy at 4 weeks that progresses to heart failure (HF) by 36 weeks. Gene profiling showed that p53 expression increases as hypertrophy worsens to HF, suggesting that p53 may influence myo-induced HF. We aimed to define how the p53 signalling cascade affects the spectrum of cardiac hypertrophy (CH)/HF.

Methods and results Immunoblot analysis showed that in myo-Tg mice (*Mus musculus*), upregulation of p53 occurs only when hypertrophy transitions to HF (16 weeks onward). To elucidate the role of p53, a double-Tg mouse line ($p53^{-/-}$/$myo^{+/+}$) was developed by crossing myo-Tg mice with p53-null mice. A significant reduction in cardiac mass with improved cardiac function was observed in $p53^{-/-}$/$myo^{+/+}$ mice, suggesting that absence of p53 prevents hypertrophy from turning into HF. Analysis via real-time reverse-transcription PCR revealed changes in transcripts of the p53 pathway in $p53^{-/-}$/$myo^{+/+}$ mice. Ingenuity Pathway Analysis™ indicated that cross-talk among several key nodal molecules (e.g. cyclin-dependent kinase inhibitor 1A, caspase-3, nuclear factor kappa-light-chain enhancer of activated B cells etc.) may play a regulatory role in the transition of CH to HF.

Conclusion Our data provide evidence, for the first time, that the coherence of p53 with myo plays an active role during the transition of CH to HF in a model of HF induced by myo overexpression. Transition from CH to HF can be prevented in the absence of p53 in myo-induced hypertrophy. Therefore, deletion/inhibition of p53 could be a therapeutic strategy to prevent CH from transitioning to HF.

Keywords Myotrophin • p53 • Cardiac hypertrophy • Heart failure

1. Introduction

Heart failure (HF) is a major cause of morbidity and mortality worldwide.[1] Prolonged cardiac hypertrophy (CH), an adaptive response the heart makes to maintain cardiac function, often precedes and sometimes finally leads to HF.[2] The mechanisms that trigger the transition of CH to HF are not fully known. Elevated levels of p53 expression have been reported to be associated with human HF in certain cases.[3,4] Leri *et al.*[5] demonstrated an association of p53 upregulation with HF. The involvement of p53 in cancer, related to tumour suppression, DNA damage, oncogenic signalling, etc. is well documented.[6] Only a few reports detail the involvement of p53 in CH and HF including elevated p53 expression in dilated cardiomyopathy.[3] The association of increased p53 expression has been reported not only in the setting of human HF but also in other cases, such as congestive HF induced by chemotherapeutic drugs,[7] pacing-induced ischaemia and myocardial infarction in rats,[8] and CH in response to pressure overload.[4,9] Most importantly, Sano *et al.*[2] suggested that the accumulation of p53 is essential for the transition from CH to HF.

Although increased levels of p53 expression have been reported, not much is known regarding p53's mechanism of action during CH and HF. Myotrophin (myo), a 12-kDa ankyrin-repeat protein, is established as one of the factors responsible for the initiation of CH that transits to HF.[10–12] Overexpression of myo in the hearts of transgenic

† Present address. Cardiovascular Research Institute, Texas A & M Health Science Center, 1901 South First Street, Temple, Texas 76504, USA.

‡ Present address. Department of Zoology, Calcutta University, 35 Ballygunge Circular Road, Calcutta 700019, India.

* Corresponding author. Tel: +1 216 444 2056; fax: +1 216 444 3110, Email: sens@ccf.org

(myo-Tg) mice causes initiation of CH at a very early age (4 weeks), and the condition progressively worsens to HF, showing symptoms that mimic the symptoms of human HF.[11,13] In this myo-Tg mouse model, upregulation of several apoptotic genes, as well as upregulation of cell regeneration candidates, has revealed that cell death and regeneration occur simultaneously during end-stage HF.[13]

Affymetrix gene array profiling of myo-Tg mice showed a 3.1-fold upregulation of a p53 homolog (AI843106) during the transition of hypertrophy to HF.[11] This finding indicates that p53 is involved in myo-induced CH/HF. The question remains whether elevated levels of p53 are associated only with the time of transition of CH to HF, as suggested by Sano *et al.*,[2] or whether these high levels are also involved earlier, in the initiation and progression of the disease process. Moreover, the possible therapeutic strategy of inhibiting p53 to prevent the transition of CH to HF[2] has not yet been reported. The success of this strategy in turn may open up the possibility of improving systolic dysfunction caused by increased cardiac p53 activity generated by various other stimuli.[2,14]

Here we report data providing that p53 plays an important role in myo-induced CH that transits to HF. To validate the therapeutic strategy of inhibition or deletion of p53 in prevention or treatment of HF, we developed a double-Tg mouse, deficient in p53 in the setting of overexpression of myo in the heart. Our data indicate that inhibiting p53, a potential therapeutic target, will reduce the occurrence of HF that is brought about by an excess of myo. The systolic dysfunction generated by various other stimuli may also be treated in this manner.[2,14]

2. Methods

2.1 Animals used

Animals required (*Mus musculus* and *Rattus norvegicus*) for the proposed study were housed and cared for in the AAALAC-approved animal facilities of the Cleveland Clinic, and all the studies conformed with the Guide for the Care and Use of Laboratory Animals published by the US National Institute of Heath (NIH Publication No. 85-23, revised 1996). All animal studies were approved by the Institutional Animal Care and Use Committee.

To evaluate p53 expression levels and other experiments, we used the following different hypertrophy/HF mouse models and their cardiac tissues: (i) myo-Tg (myo$^{+/+}$) mice,[11,13] (ii) the transverse aortic constriction (TAC) model,[15] (iii) for conditional overexpression of myo in a cardiac-specific manner, we used tetracycline (Tet) controlled binary myo-Tg mice, and (iv) p53-null (p53$^{-/-}$) mice[16] (see Supplementary material online, Methods).

2.2 Human tissue

We have also compared non-failing and failing human heart tissue to evaluate p53 expression levels. The investigation conforms with the principles outlined in the Declaration of Helsinki. Collection of tissues and other related protocols for tissue procurement were approved by Cleveland Clinic's Institutional Review Board, as mentioned previously[17] (see Supplementary material online, Methods). Left ventricular tissues used in the experiments were the same as those described earlier.[17]

2.3 Preparation of neonatal rat ventricular myocytes

Neonatal rat (*Rattus norvegicus*) ventricular cardiomyocytes were isolated from 3- to 4-day-old American Wistar rat pups according to the procedure described by Sen *et al.*[10]

2.4 Confocal imaging to detect activation of p53 by myo and quantitation of cell surface area

Isolated rat neonatal ventricular myocytes were stimulated with myo and 5-fluorouracil (5-FU, a potent activator of p53)[18] for 24 h; cell fixation and permeabilization and confocal imaging was performed as described previously[12,19] (see Supplementary material online, Methods). Stimulation of cardiomyocytes with 100 nm Angiotensin II (Sar^{1})[20] was performed as positive control for the measurement of cell surface area using Image-Pro Plus 6.1 software (see Supplementary material online, Methods).

2.5 Generation of double-Tg lines and determination of their genotyping

We developed our p53$^{-/-}$/myo$^{+/+}$ double-Tg line by breeding myo$^{+/+}$ and p53$^{-/-}$ mice (see Supplementary material online, Methods). We also performed breeding of FVB-wild-type (WT) and BL-6 WT mice to generate crossbred FVB/BL-6 WT mice for our study because the parental background of the myo-Tg and p53$^{-/-}$ mice are FVB and BL-6, respectively.

2.6 Measurement of heart weight:body weight ratio

The heart weight:body weight (HW:BW) ratio (mg/g) was determined according to the protocol of Sarkar *et al.*[11] Three individual mice in each group were studied.

2.7 Histology

Paraffin-embedded mice heart sections were stained for haematoxylin/eosin and Masson's trichrome using standard techniques (see Supplementary material online, Methods).

2.8 Determination of cardiac function by echocardiography

Two-dimensional echocardiography was performed at the Department of Cardiovascular Medicine, Cleveland Clinic, following the protocol of Peng *et al.*[21]

2.9 RNA isolation and reverse transcription PCR for gene expression profiling

Total RNA was isolated and reverse transcription (RT) PCR analysis was performed following the protocol described previously[12] (see Supplementary material online, Methods).

2.10 p53 real-time reverse transcriptase PCR pathway array

A real-time reverse transcriptase polymerase chain reaction (RT^{2}-PCR) array was performed at SuperArray Biosciences Corp. (Frederick, MD) for p53 signalling pathway analyses in myo-Tg and p53$^{-/-}$/myo$^{+/+}$ mice using the RNA obtained from the heart tissues (see Supplementary material online, Methods).

2.11 Ingenuity Pathway Analysis^{TM} for generating the functional network

On the basis of cut-off value (fold increase/decrease) of 2, selected candidate genes obtained from the RT^{2}-PCR array were used as focus molecules subjected to the Ingenuity Pathway Analysis^{TM} (IPA) functional network[22] (see Supplementary material online, Methods). From this functional network, nodal molecules were selected for their validation and to postulate the functional role.

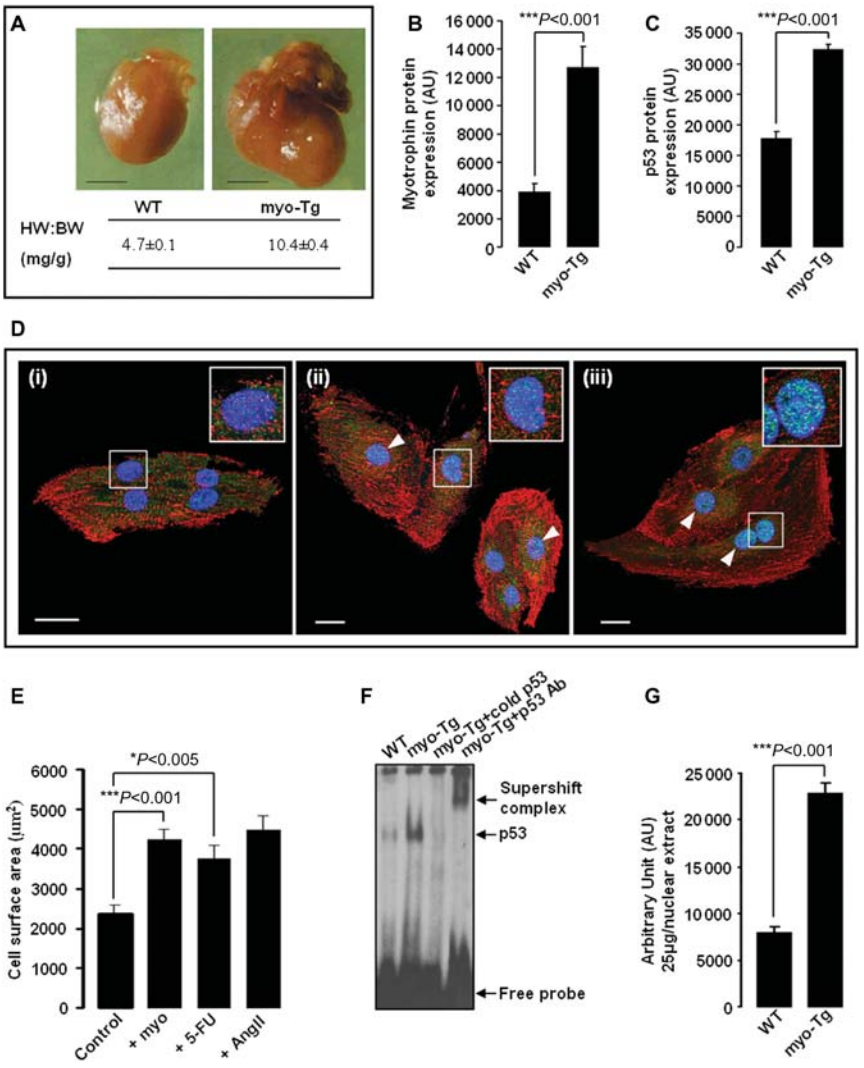

Figure 1 Myotrophin (myo)-induced heart failure (HF) in 36-week-old myo-Tg mice is associated with elevated expression of p53 and activation of p53 by myo, stimulating cardiac cell growth. (*A*) Overexpression of myo in the hearts of myo-Tg mice results in enlarged hearts and increased HW:BW ratio compared with age-matched wild-type (WT) mice during HF (>36 weeks) (black bar represents 10 mm); (*B*) A significant ($P < 0.001$) increase in myo protein in 36-week-old myo-Tg mice; (*C*) Elevated level of p53 protein in 36-week-old myo-Tg mice; (*D*) Confocal micrographs (×63) of neonatal rat cardiomyocytes immunostained for p53 (AlexaFluor®488-green/cyan), for sarcomeric α-actinin (AlexaFluor®568-red), and for nucleus (DAPI, blue). Neonatal rat cardiomyocytes [panel (i) is unstimulated] showed increased nuclear localization of p53 (white arrowhead) after treatment with myo (panel ii) and 5-FU (panel iii). The two-fold enlarged view of a single nucleus appears in the inset (white bar represents 20 μm); (*E*) Neonatal rat cardiomyocytes, stimulated with myo and 5-FU showing significant (Bonferroni's corrected $P < 0.001$ and $P < 0.05$, respectively) increase in cell surface area compared with untreated control cells. Ang II stimulation was performed as positive control. The data (mean ± SEM) for each group is an average of nine individual measurements; (*F*) EMSA showing increased activation of p53 in myo-Tg mice compared with WT mice; (*G*) Quantification of EMSA showing significant ($P < 0.001$) increase in p53 activation in myo-Tg mice compared with WT mice. Values obtained from three independent experiments are expressed as arbitrary units (AU). [Data for (*A*) and (*B*) were adapted from Sarkar *et al.*[11] and Gupta *et al.*[38]].

2.12 Protein isolation and immunoblot analysis for protein expression profiling

Total protein was isolated from left ventricular tissues (from three independent individuals in each case) and immunoblot analysis was done following the protocol described previously.[17] Expression levels were quantified with NIH ImageJ software, and obtained values were expressed in arbitrary units.

2.13 Nuclear protein extraction and electrophoretic mobility shift assay

Nuclear protein extraction from WT and Tg mouse hearts (three individuals in each experiment for each group) and electrophoretic mobility shift assay (EMSA) were performed following the protocol described earlier[23–25] (see Supplementary material online, Methods).

2.14 Statistical analysis

Results obtained in individual experiments were expressed as mean ± SEM. A Student's *t*-test was performed to determine the statistical significance. Differences between more than two experimental groups were evaluated for statistical significance either by one-way analysis of variance (ANOVA) or by two-way ANOVA (for p53 expression of WT and $p53^{-/-}$/$myo^{+/+}$ mice at various ages) with Bonferroni's post tests using

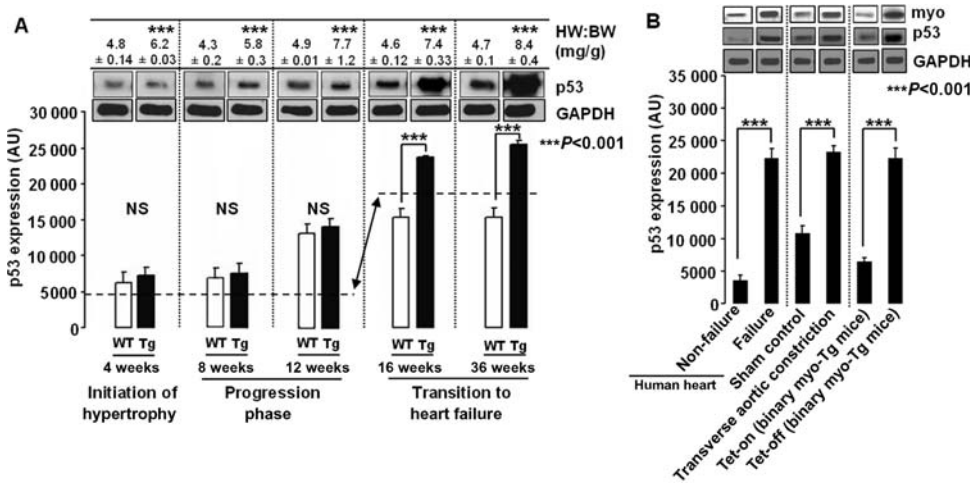

Figure 2 Increase in p53 expression during transition of CH to HF. (*A*) Immunoblot analysis of p53 in myo-Tg mice showing significant (Bonferroni's corrected $P < 0.001$) upregulation (↔) of p53 expression from 16 weeks of age compared with wild-type (the start of the transition to HF, although HW:BW ratio shown in the upper panel indicates that CH starts at 4 weeks); (*B*) Immunoblot analysis showing elevated expression of p53 (Bonferroni's corrected $P < 0.001$) in failing human heart, in the TAC mouse model, and in Tet-control binary Tg mice along with myo expression. Results are presented as mean ± SEM and represent three independent experiments. (GAPDH was used as a loading control).

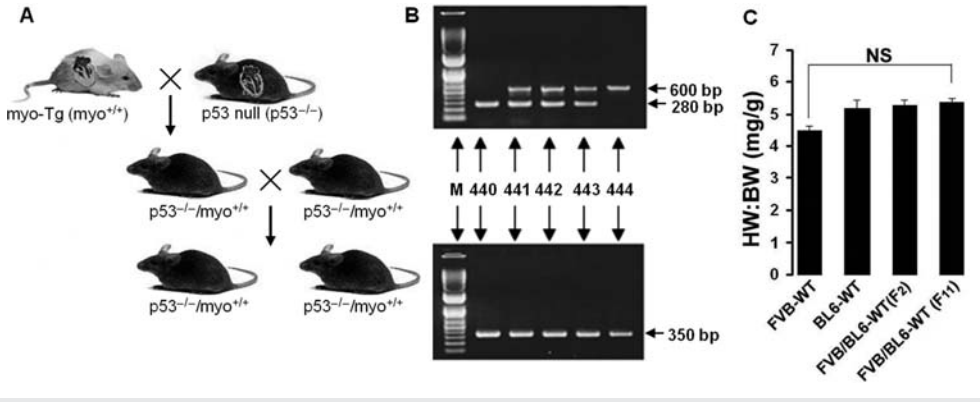

Figure 3 Generation of double-transgenic mice. (*A*) Breeding strategy showing generation of $p53^{-/-}/myo^{+/+}$ double-Tg mice in filial generation from Tg mice overexpressing myotrophin in the heart (myo-Tg, i.e. $myo^{+/+}$) and p53-null ($p53^{-/-}$) parents; (*B*) Genotyping of filial offspring by using specific sets of primers (as mentioned in the text) to identify $p53^{-/-}/myo^{+/+}$ (no. 440), $p53^{+/-}/myo^{+/+}$ (no. 441, 442, 443), and $p53^{+/+}/myo^{+/+}$ (no. 444) individuals (amplicon at 600 and 280 bp are for p53 and at 350 bp is for myo); (*C*) No significant (NS; Bonferroni's corrected $P > 0.05$) changes in HW:BW ratio among WT FVB, BL6 and crossbred FVB/BL6-WT mice in subsequent generations (F2 and F11 documented here), showing no changes in cardiac mass due to cross-breeding of two different parental backgrounds of the double-Tg mice. Results are presented as mean ± SEM and represent three independent experiments.

GraphPad Prism 4.0 software (GraphPad software, San Diego, CA, USA). Differences were considered significant at $P < 0.05$.

3. Results

3.1 Elevated expression of myo and p53 during HF

Cardiac-specific overexpression of myo in myo-Tg mice resulted in increased HW:BW ratio (10.4 ± 0.4 mg/g) and enlargement of the heart compared with age-matched WT mice (4.7 ± 0.1 mg/g) during HF (*Figure 1A*). Increased expression of myo protein in 36-week-old myo-Tg mice (*Figure 1B*) was found to be associated with elevated levels of p53 protein expression (*Figure 1C*).

3.2 Activation of p53 by myo

To study the involvement of p53 and the specificity of p53 in myo-induced CH that transits to HF, *in vitro* experiments were performed. Isolated neonatal rat cardiomyocytes were stimulated with myo (40 μM) and with 5-FU (20 μg/mL) in separate experimental sets. Confocal micrography of immunostained unstimulated and stimulated cells showed that there was an increase in the expression

and nuclear localization of p53 molecules in both myo-stimulated and 5-FU-stimulated cells compared with unstimulated cells (*Figure 1D*). Significant increases in cell surface area ($P < 0.001$ and $P < 0.05$) in stimulated cells (*Figure 1E*) confirmed that the above-mentioned stimulation resulted in cell growth. Furthermore, p53 EMSA profile (*Figure 1F*) of WT and myo-Tg mice showed a significant increase ($P < 0.001$) in the activation of p53 in myo-Tg mice compared with WT mice (*Figure 1G*). Thus, p53 expression and activation have been proved to be induced directly by myo.

3.3 Changes in p53 expression during progression of CH to HF

To determine at what phases—initiation, progression, or transition of CH to HF—p53 expression becomes altered, we quantified p53 levels in myo-Tg and age-matched WT mice at 4, 8, 12, 16 and 36 weeks of age, these ages representing different phases of the disease, as described earlier.[11] At the initiation phase of CH (4 weeks) and during the progression phase of the disease (8 and 12 weeks), despite having hypertrophy, as indicated by a significant ($P < 0.001$) increase in HW:BW ratio in myo-Tg mice compared with age-matched WT mice, p53 expression levels remained unaltered (no significant changes between WT and myo-Tg, $P > 0.05$, *Figure 2A*). Time-dependent significant changes ($P < 0.001$) for p53 expression started at 12 weeks, but the changes were observed both in WT and Tg mice. Changes in HW:BW ratio continued to increase beginning at 16 and 36 weeks of age. The period between these two points represent the transition phase of CH to HF. p53 expression levels suddenly elevated significantly ($P < 0.001$) and continued to increase beginning in this transition phase (from 16 weeks onward) in myo-Tg mice compared with age-matched WT mice (*Figure 2A*). This increase indicates that the elevation of p53 occurs only at the point when chronic CH worsens to HF, not at the initiation or progression phases of the disease.

3.4 Elevated levels of p53 and myo in human HF and in a murine HF model

To evaluate the correlation between changes in p53 and myo expression levels with HF, we examined the p53 expression profile in non-failing and failing human hearts and in a TAC mouse model of experimentally induced HF where we have shown increased myo expression (*Figure 2B*).[26,27] Levels of p53 expression were found to be elevated significantly ($P < 0.001$) in failing human heart and in TAC mice compared with non-failing hearts and sham control, respectively (*Figure 2B*).

3.5 Alteration of p53 expression parallels myo gene expression

We also studied the effect of alteration of myo gene expression on p53 expression in our Tet control binary myo-Tg mouse model. In the binary myo-Tg mice, myo expression is controlled with a cardiac-specific Tet-responsive system (Tet-on/Tet-off), where gene expression initiation was achieved by removing doxycycline from the drinking water (S. Gupta and S. Sen, unpublished results). A significant ($P < 0.001$) increase in HW:BW ratio (5.56 ± 0.27 mg/g) was observed in Tet-off (myo gene on) binary Tg mice compared with HW:BW ratio (4.52 ± 0.28 mg/g) of Tet-on (myo gene-off) binary Tg mice. This increase was associated with increased levels of myo protein expression (*Figure 2B*). We found that when the myo gene was expressed, there were elevated levels of p53 protein compared with Tet-on binary myo-Tg mice, in which the myo gene is turned off (*Figure 2B*). Thus, there is a correlation between myo gene expression and elevated levels of p53 protein expression.

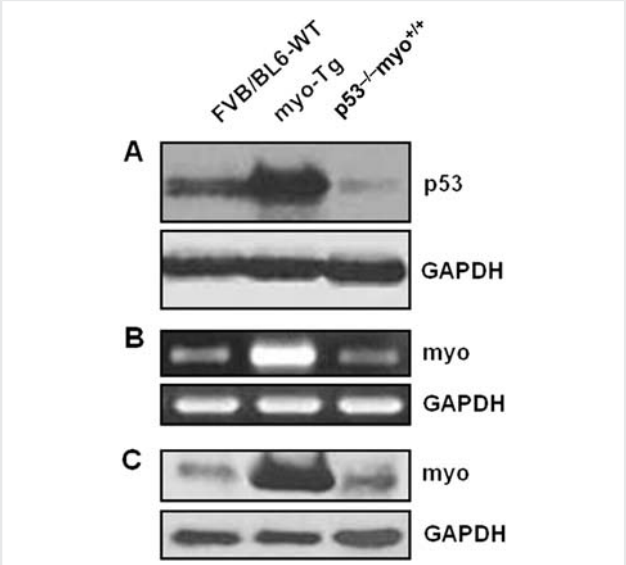

Figure 4 Reduced expression of p53 in $p53^{-/-}/myo^{+/+}$ mice is correlated with myotrophin expression. (*A*) Immunoblot analysis of p53 showing downregulation of p53 in $p53^{-/-}/myo^{+/+}$ mice compared with myo-Tg mice; (*B*) Semi-quantitative RT-PCR analysis showing downregulation of myo transcript in $p53^{-/-}/myo^{+/+}$ mice compared with myo-Tg mice; (*C*) Immunoblot analysis of myo protein showing reduced expression of myo in the absence of p53 in $p53^{-/-}/myo^{+/+}$ mice compared with myo-Tg mice. (GAPDH was analysed as a loading control).

3.6 Generation of double-Tg mice and expression of p53 and myo

To test the hypothesis that in the absence of p53, myo-induced CH failed to worsen to HF, we generated double-Tg mouse lines ($p53^{-/-}/myo^{+/+}$) by breeding our previously reported myo-Tg ($myo^{+/+}$) mice[11] with p53-null ($p53^{-/-}$) mice[16] (*Figure 3A* and *B*). The filial individuals obtained from these breedings possess various heterozygous/homozygous genotypes in typical Mendelian fashion throughout several consecutive generations (*Figure 3A* and *B*). The obtained double-Tg $p53^{-/-}/myo^{+/+}$ mice are p53 null with a myo overexpression background. We have also generated FVB/BL-6 crossbred WT mice by breeding FVB WT with BL-6 WT mice, as myo-Tg ($myo^{+/+}$) mice have an FVB parental background and p53-null ($p53^{-/-}$) mice have a BL-6 background. The HW:BW ratio in all types of WT mice used (FVB, BL-6, and FVB/BL-6 crossbred) showed no significant changes (Bonferroni's corrected value of $P > 0.05$), indicating that differences in parental background does not affect cardiac mass (*Figure 3C*). The $p53^{-/-}/myo^{+/+}$ mice, before developing tumours due to the p53-null condition, were analysed at 16 weeks of age, which is the point of transition of CH to HF phase. p53 expression profiling of both $p53^{-/-}/myo^{+/+}$ mice and FVB/BL6-WT mice showed reduced levels of p53 expression compared with myo-Tg mice (*Figure 4A*). Myo expression, at both the

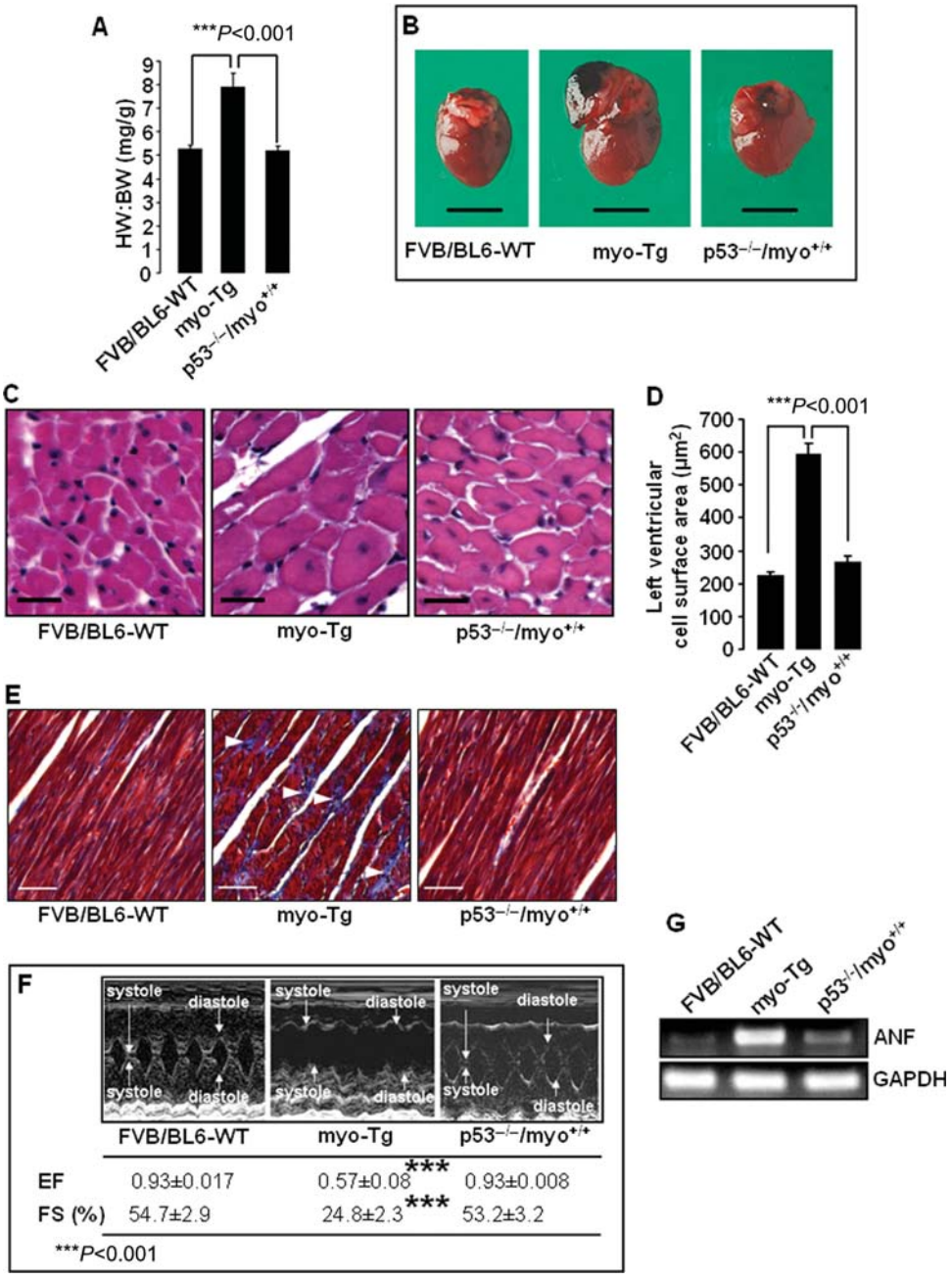

Figure 5 Absence of p53 in $p53^{-/-}/myo^{+/+}$ double Tg mice resulted in the regression of cardiac mass associated with improved cardiac function. (*A*) HW:BW ratios showing significant (Bonferroni's corrected $P < 0.001$) reduction in cardiac mass in $p53^{-/-}/myo^{+/+}$ mice compared with myo-Tg mice. The results are presented as mean ± SEM and represent three independent experiments. (*B*) Hearts from 16-week-old FVB/BL6-WT, myo-Tg, and $p53^{-/-}/myo^{+/+}$ mice; (*C*) Haematoxylin–eosin stained cells from left ventricles of FVB/BL6-WT, myo-Tg, and $p53^{-/-}/myo^{+/+}$ mice (×20 magnification, white bar represents 25 μm); (*D*) Measurement of left ventricular cell surface area showing significantly enlarged cell (Bonferroni's corrected $P < 0.001$) in myo-Tg mice compared with FVB/BL6-WT and $p53^{-/-}/myo^{+/+}$ mice. Data (mean ± SEM) for each group is an average of nine individual measurements; (*E*) Masson's trichrome staining of the left ventricle demonstrates collagen deposition (white arrowhead) in myo-Tg mice (×20 magnification, white bar represents 50 μm); (*F*) M-mode echocardiography showing improved cardiac function in $p53^{-/-}/myo^{+/+}$ mice, where values for both ejection fraction (EF) and fractional shortening (FS) increased significantly (Bonferroni's corrected $P < 0.001$) compared with myo-Tg mice and are almost identical to those of WT mice; (*G*) RT-PCR analysis showing downregulation of the hypertrophic marker gene atrial natriuretic factor (ANF) in $p53^{-/-}/myo^{+/+}$ mice. In RT-PCR analysis, GAPDH was analysed as a loading control.

Table 1 Candidate molecules of the p53 pathway obtained by p53 RT^2-PCR pathway array

Gene symbol	GenBank ID	Gene description	Mean fold changes
Upregulated genes			
Apex1	NM_009687	Apurinic/apyrimidinic endonuclease 1	2.86
Bag1	NM_009736	Bcl2-associated athanogene 1	2.14
ccng1	NM_009831	Cyclin G1	2.53
Cradd	NM_009950	CASP2 and RIPK1 domain containing adaptor with death domain	2.10
Gadd45a	NM_007836	Growth arrest and DNA-damage-inducible 45 alpha	3.36
Msh2	NM_008628	MutS homolog 2 (*Escherichia coli*)	2.29
Pttg1	NM_013917	Pituitary tumour-transforming 1	17.85
Rprm	NM_023396	Reprimo, TP53-dependent G2 arrest mediator candidate	2.92
Sfn	NM_018754	Stratifin	5.97
Xrcc5	NM_009533	X-ray repair complementing defective repair in Chinese hamster cells 5	2.03
Downregulated genes			
Apaf1	NM_009684	Apoptotic peptidase activating factor 1	2.13
Bcl2	NM_009741	B-cell leukaemia/lymphoma 2	3.25
Bid	NM_007544	BH3 interacting domain death agonist	2.45
Brca1	NM_009764	Breast cancer 1	2.16
Cdc2a	NM_007659	Cell division cycle 2 homolog A (*Schizosaccharomyces pombe*)	2.55
Cdkn1a	NM_007669	Cyclin-dependent kinase inhibitor 1A (P21)	2.85
E2f1	NM_007891	E2F transcription factor 1	2.00
FasL	NM_010177	Fas ligand (TNF superfamily, member 6)	2.61
IL6	NM_031168	Interleukin 6	13.66
Myc	NM_010849	Myelocytomatosis oncogene	4.73
Pmaip1	NM_021451	Phorbol-12-myristate-13-acetate-induced protein 1	2.66
Traf1	NM_009421	Tnf receptor-associated factor 1	2.91
Vcan	XM_488510	Versican	3.19
wt1	NM_144783	Wilms tumour homolog	2.03

Selected up- and downregulated transcripts of the p53 pathway in p53$^{-/-}$/myo$^{+/+}$ mice (fold changes over myo-Tg mice) based on a cut-off value of 2. Values are expressed as the mean of fold changes from three independent experiments.

transcript and protein level, was also reduced in the absence of p53 in p53$^{-/-}$/myo$^{+/+}$ mice (*Figure 4B* and *C*).

3.7 Reduction in cardiac mass and improvement of cardiac function in the absence of p53

Significant ($P < 0.001$) reduction in the HW:BW ratio was observed in p53$^{-/-}$/myo$^{+/+}$ mice (5.2 $\pm$ 0.21 mg/g) compared with myo-Tg mice (7.9 $\pm$ 0.58 mg/g) (*Figure 5A*). The values obtained for p53$^{+/-}$/myo$^{+/+}$ mice were between those of the myo-Tg and p53$^{-/-}$/myo$^{+/+}$ mice, and all WT mice were in the same range of values, which were much lower than those of the myo-Tg mice (data not shown). Reduction in heart size (*Figure 5B*) was observed in p53$^{-/-}$/myo$^{+/+}$ mice. Enlargement of the left ventricular cell, which was observed in myo-Tg mice compared with FVB/BL6-WT, reduced significantly ($P < 0.001$) in p53$^{-/-}$/myo$^{+/+}$ mice (*Figure 5C* and *D*). Furthermore, deposition of collagen fibre, present in myo-Tg mice, were absent in p53$^{-/-}$/myo$^{+/+}$ mice (*Figure 5E*). All these observations indicated that even in the condition of myo overexpression, hypertrophy did not develop because of the absence of p53 in p53$^{-/-}$/myo$^{+/+}$ mice. In addition to reduction in cardiac mass, cardiac function in p53$^{-/-}$/myo$^{+/+}$ mice improved significantly (Bonferroni's corrected value of $P < 0.001$) compared with myo-Tg mice, as observed in echocardiographic analysis (*Figure 5F*, see Supplementary material online, *Table S1*). Particularly, fractional shortening and ejection fraction values of the p53$^{-/-}$/myo$^{+/+}$ mice became similar to those of WT mice. Therefore, our data showed that in the absence of p53, even in mice engineered to overexpress myo, cardiac function remains similar to that of WT mice. Furthermore, downregulation of atrial natriuretic factor, a hypertrophy marker gene (*Figure 5G*), indicated the prevention of hypertrophy in the p53$^{-/-}$/myo$^{+/+}$ mice.

3.8 Involvement of the p53 signalling cascade in the transition of CH to HF

To further confirm the participation of p53 signalling in CH and HF, we performed RT^2-PCR profiling of the p53 signalling pathway in p53$^{-/-}$/myo$^{+/+}$ and myo-Tg mice. Analysis of the RT^2-PCR p53 pathway array showed that a total of 24 gene products were up- or downregulated (10 upregulated and 14 downregulated) based on the cut-off value 2 in p53$^{-/-}$/myo$^{+/+}$ mice compared with myo-Tg mice (*Table 1*). We have used these selected genes as focus molecules with which to build an IPA^{TM} functional network. The IPA^{TM} Knowledge Base generated the functional network (*Figure 6*) by including 18 focus molecules. In addition to these, the network selected related molecules from the Knowledge Base for a total of 49 network participants. Of these 49 network participants, five molecules (caspase, NF-κB, Myc, Bcl2, and Cdkn1a) were generated as nodal molecules

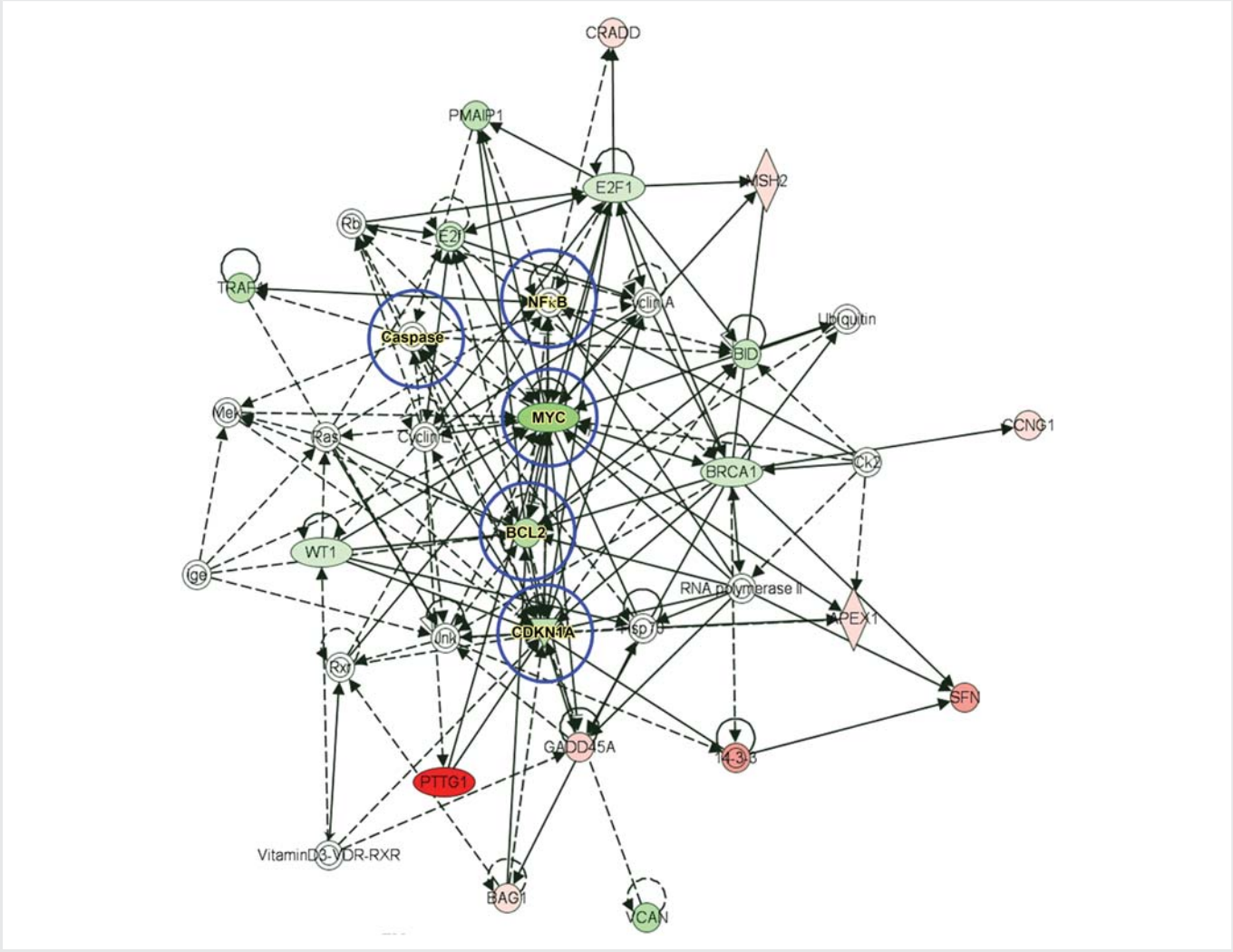

Figure 6 IPA™ functional network as generated by focus molecules. Selected upregulated (shades of red) and downregulated (shades of green) candidate molecules, obtained from an RT^2-PCR p53 pathway array, were used as focus molecules to generate the functional network. Candidate molecules not shaded by any colour were generated by the network from its knowledge base. IPA-predicted nodal molecules, which can regulate the entire network, are circled in blue. Solid arrows between molecules depict experimentally proven relationships. Dashed lines depict inferred interactions based on experimental evidence.

that play a central role; the other participant molecules are in some way related to those nodal molecules.

3.9 Involvement of IPA™-generated nodal molecules in HF

Furthermore, we have validated the participation of IPA™-generated nodal molecules, namely, Cdkn1a, Bcl2, c-*Myc*, caspase-3, and NF-κB. Immunoblot analysis showed that the levels of these nodal molecules were reduced in p53$^{-/-}$/myo$^{+/+}$ mice compared with myo-Tg mice (*Figure 7A*). Gel mobility shift assay revealed suppression of NF-κB activity in p53$^{-/-}$/myo$^{+/+}$ mice, whereas in myo-Tg mice, the activity was higher than in WT mice (*Figure 7B* and *C*). Changes in NF-κB activity is expected to correlate with changes in IκB-α protein level. Immunoblot analysis showed a decrease in IκB-α protein levels that is associated with suppressed NF-κB activation in p53$^{-/-}$/myo$^{+/+}$ mice compared with myo-Tg mice (*Figure 7D*).

4. Discussion

It is well established that myo triggers CH, which then transits to HF.[10,11,28] An early activation of myo during human HF was observed by O'Brien *et al.*[29] In that same study, it was reported that myo levels increased as the severity of the disease increased. In myo-Tg mice that have cardiac-specific overexpression of myo, initiation of CH occurs at a very early age (4 weeks); hypertrophy in these mice gradually worsens to HF at 36 weeks of age.[11,13] Importantly, the molecular changes observed in the hearts of myo-Tg mice are similar to those observed in other models of hypertrophy, such as TAC, the DOCA-salt model, and renal hypertensive rat.[27] Moreover, myo-Tg mice provide a murine model of HF that closely mimics symptoms of human HF.[11,13] Overexpression of myo in the myo-Tg mouse model thus allows us to study the molecular changes that occur during different phases of the disease, starting from the initiation of CH through progression of the disease and during the transition to HF.[11]

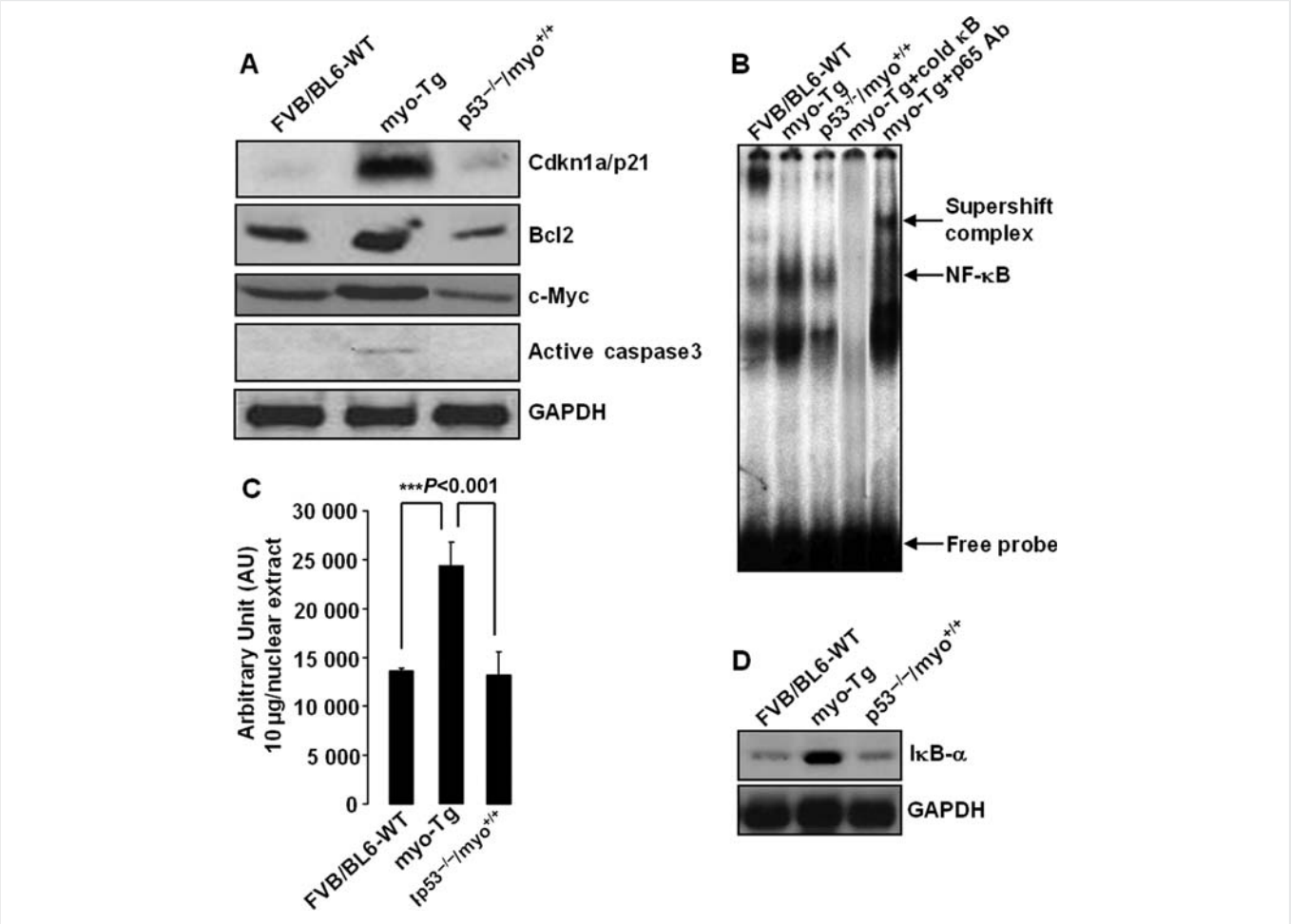

Figure 7 Expression profiles of IPA™-predicted nodal molecules. (*A*) Immunoblot analysis showing downregulation of IPA-predicted nodal molecules Cdkn1a, Bcl2, c-*Myc*, and caspase (active caspase3) in $p53^{-/-}/myo^{+/+}$ mice, revealing active participation of these molecules in the prevention of HF in the absence of p53; (*B*) EMSA showing regression of NF-κB activity in $p53^{-/-}/myo^{+/+}$ mice; (*C*) Quantification of EMSA. Values obtained from three independent experiments are expressed as arbitrary units (AU), (Bonferroni's corrected $P < 0.001$). (*D*) Immunoblot analysis showing downregulation of IκB-α protein in $p53^{-/-}/myo^{+/+}$ mice correlating the regression of NF-κB activity in the absence of p53 to prevent HF. (GAPDH was analysed as a loading control for A & D).

Affymetrix gene array profiling revealed an increase in p53 gene expression in myo-Tg mice specifically at the HF stage.[11] Thus, we hypothesized that p53 is involved in myo-induced CH that progressively leads to HF. To test our hypothesis, we performed *in vitro* experiments to determine whether or not myo stimulation involves elevated p53 expression. We previously reported that myo stimulates myocyte growth when isolated neonatal rat cardiomyocytes are treated with myo.[12] In this study, activation and increased expression of p53, associated with an increase in cell surface area and thereby cell growth, was observed in myo-stimulated neonatal rat cardiomyocytes (*Figure 1D* and *E*). This observation supports our hypothesis that p53 actively participates in myo-induced CH and HF. Furthermore, activation of p53 in myo-Tg mice (*Figure 1F* and *G*) indicated that p53 is directly regulated by myo. Other researchers have also reported participation of p53 in various forms of HF,[2,3,30] but none of the previous studies had determined the stage at which p53 participates in heart disease.

Because the myo-Tg model mimics the phenomenon of human HF,[13] we took advantage of this model to study the involvement of p53 at various phases of CH and HF. Our data clearly showed that p53 expression levels became elevated only during the transition from the CH phase to the HF stage, but not prior to that, even when there was occurrence of CH (*Figure 2A*). This observation is in accord with the earlier report of Sano *et al.*[2]; those authors suggested that the accumulation of p53 is required for the transition from CH to HF. Upregulation of p53 may insure cell-cycle arrest when cardiomyocytes are stimulated by pro-growth factors like myo, permitting cardiomyocyte hypertrophy rather than proliferation.[31] The very small change in p53 expression at 12 weeks of age compared with 4 and 8 weeks is probably due to the ageing process, as similar changes were observed in WT mice. Furthermore, we confirmed that elevated p53 expression is not restricted solely to our myo-Tg HF model; it was also evident in failing human hearts and in the TAC mouse model (*Figure 2B*). The relationship between elevated expression of p53 and myo expression was established in the Tet-control myo-binary Tg mice that conditionally overexpress myo. In these binary-Tg mice, we found that p53 protein levels increased when myo gene expression

was conditionally turned on (*Figure 2B*). Similarly, coherence of elevated level of myo and p53 was also observed in failing human hearts and TAC mice (*Figure 2B*). All these findings indicate that p53 plays an active and important role at the point of transition of CH to HF.

As p53 was found to be involved during the process of CH and HF, we hypothesized that a lack of p53 might improve cardiac function and inhibit the transition to HF. We therefore generated the $p53^{-/-}/myo^{+/+}$ double-transgenic mice (*Figure 3A* and *B*). In these mice, compared with myo-Tg mice, cardiac mass and cardiac cell size were reduced significantly, and cardiac function was improved (*Figure 5A–F*). This implies that p53 should be a relevant therapeutic target for the treatment of HF, as has been proposed previously.[14,32] The fact that hypertrophy did not develop in the absence of p53 appears to be due to inhibition of myo expression.

Although we have demonstrated the involvement of p53 in CH and HF, the intricate signalling cascade that is presumably involved remains to be fully explored. A combination of transcriptional profiling and IPA™ analysis provides the opportunity for mechanistic studies.[33,34] Transcriptional profiling of myo-Tg and $p53^{-/-}/myo^{+/+}$ mouse hearts using an RT^2-PCR pathway array revealed the involvement of several p53 pathway members in the disease process.

The IPA™ functional network, generated using candidates obtained from transcriptome profiling, revealed the involvement of the regulator of cell cycle progression protein Cdkn1a/p21, anti-apoptotic protein Bcl2, and apoptotic effector protein caspases as nodal molecules (*Figure 6*). These nodal molecules were downregulated in $p53^{-/-}/myo^{+/+}$ mice compared with myo-Tg mice (*Figure 7A*), suggesting active participation in the regulation of cardiac function. This observation supports our previous findings that both cell death and cell regeneration occur simultaneously during the transition of hypertrophy to HF.[13]

The Bcl2 family of proteins is regulated by p53,[35] and elevated levels of Bcl2 in patients with HF have been reported by Olivetti *et al.*[36] Upregulation of Bcl2 in response to HF induced by pressure overload has also been documented.[37] Here we observed downregulation of Bcl2 (*Figure 7A*) in the absence of its regulator protein p53, confirming that the deletion or blocking of p53 can inhibit/prevent the transition of the hypertrophic process to HF.

Interestingly, the IPA™ software predicted that NF-κB is one of the nodal molecules involved in p53-related CH and HF. Activation of NF-κB, particularly in myo-induced hypertrophy, is necessary for the induction of CH that leads to HF.[24,38] We have shown that NF-κB-stimulated myocyte growth is regulated by interaction and nuclear co-translocation of myo and NF-κB-p65.[12] NF-κB and p53 proteins share similarities in their structure, DNA binding, and regulation by ankyrin-repeat proteins.[39] Myo is an ankyrin-repeat protein and may regulate p53, as it regulates NF-κB-p65, during the CH process. Under certain conditions, NF-κB activation occurs simultaneously with the induction of Cdkn1a/p21, a principal target of p53.[40] Apart from its participation in myo-induced CH, NF-κB generally promotes resistance to programmed cell death.[41–43] Conversely, p53 induces apoptosis or cell-cycle arrest.[44,45] However, p53 can indirectly stimulate NF-κB through induction of Cdkn1a/p21.[40] During the transition of CH to HF, elevated levels of p53 activate NF-κB and a high level of NF-κB activation is obtained at the time of transition to HF. On the basis of this putative regulatory mechanism, repression of NF-κB activation should occur, as confirmed in our study (*Figure 7B* and *C*), in the absence of p53, a condition that is reflected in improved cardiac function and regression of cardiac mass in $p53^{-/-}/myo^{+/+}$ mice.

The major new finding of this study is that, in the absence of p53, CH (which usually transits to HF in our model of murine HF) was prevented from occurring. Although the possible mechanisms involving p53, NF-κB, and other nodal molecules such as Bcl2 in the transition to HF require further detailed study, data obtained from this investigation clearly suggest that deletion/inhibition of p53 can prevent or minimize the occurrence of HF. It is evident that the elevation of p53 expression occurs only during the transition of CH to HF, but not prior to that; thus, therapeutically inhibiting p53 at the initiation of transition phase (12–16 weeks in myo-Tg mice) may prevent or delay the onset of HF in patients as well.

Supplementary material

Supplementary material is available at *Cardiovascular Research* online.

Acknowledgements

The authors acknowledge Sathyamangala V. Naga Prasad, PhD (Department of Molecular Cardiology, LRI, Cleveland Clinic), for providing BL6 and TAC mice; Nikolai Sopko, PhD (Department of Stem Cell Biology and Regenerative Medicine, LRI, Cleveland Clinic) for discussion with the hemodynamic data analysis; Christine S. Moravec, PhD (Director of Basic Research, Kaufman Center for Heart Failure, Cleveland Clinic), of the heart transplant team for providing the human heart tissues and Ms Linda Vargo (Imaging Core, Lerner Research Institute, Cleveland Clinic) for assistance in histological preparations.

Conflict of interest: none declared.

Funding

This work was supported by a grant from the National Institutes of Health [HL R01 47794] to S.S.

References

1. Braunwald E, Bristow MR. Congestive heart failure: fifty years of progress. *Circulation* 2000;**102**:IV14–IV23.
2. Sano M, Minamino T, Toko H, Miyauchi H, Orimo M, Qin Y *et al.* p53-induced inhibition of Hif-1 causes cardiac dysfunction during pressure overload. *Nature* 2007;**446**:444–448.
3. Birks EJ, Latif N, Enesa K, Folkvang T, Luong lASarathchandraP *et al.* Elevated p53 expression is associated with dysregulation of the ubiquitin–proteasome system in dilated cardiomyopathy. *Cardiovasc Res* 2008;**79**:472–480.
4. Tsukamoto O, Minamino T, Okada K, Shintani Y, Takashima S, Kato H *et al.* Depression of proteasome activities during the progression of cardiac dysfunction in pressure-overloaded heart of mice. *Biochem Biophys Res Commun* 2006;**340**:1125–1133.
5. Leri A, Franco S, Zacheo A, Barlucchi L, Chimenti S, Limana F *et al.* Ablation of telomerase and telomere loss leads to cardiac dilatation and heart failure associated with p53 upregulation. *EMBO J* 2003;**22**:131–139.
6. Efeyan A, Serrano M. p53: guardian of the genome and policeman of the oncogenes. *Cell Cycle* 2007;**6**:1006–1010.
7. Venkatakrishnan CD, Dunsmore K, Wong H, Roy S, Sen CK, Wani A *et al.* HSP27 regulates p53 transcriptional activity in doxorubicin-treated fibroblasts and cardiac H9c2 cells: p21 upregulation and G2/M phase cell cycle arrest. *Am J Physiol Heart Circ Physiol* 2008;**294**:H1736–H1744.
8. Oie E, Clausen OP, Yndestad A, Grogaard HK, Attramadal H. Endothelin receptor antagonism attenuates cardiomyocyte apoptosis after induction of ischemia in rats. *Scand Cardiovasc J* 2002;**36**:108–116.
9. Ikeda S, Hamada M, Hiwada K. Cardiomyocyte apoptosis with enhanced expression of P53 and Bax in right ventricle after pulmonary arterial banding. *Life Sci* 1999;**65**:925–933.
10. Sen S, Kundu G, Mekhail N, Castel J, Misono K, Healy B. Myotrophin: purification of a novel peptide from spontaneously hypertensive rat heart that influences myocardial growth. *J Biol Chem* 1990;**265**:16635–16643.

11. Sarkar S, Leaman DW, Gupta S, Sil P, Young D, Morerhead A *et al*. Cardiac expression of myotrophin triggers myocardial hypertrophy and heart failure in transgenic mice: Changes in gene expression profiles during initiation of hypertrophy and during heart failure measured by DNA microarray analysis. *J Biol Chem* 2004;**279**: 20422–20434.
12. Das B, Gupta S, Vasanji A, Xu Z, Misra S, Sen S. Nuclear co-translocation of myotrophin and p65 stimulates myocyte growth: regulation by myotrophin hairpin loops. *J Biol Chem* 2008;**283**:27947–27956.
13. Sarkar S, Chawla-Sarkar M, Young D, Nishiyama K, Rayborn ME, Hollyfield JG *et al*. Myocardial cell death and regeneration during progression of cardiac hypertrophy to heart failure. *J Biol Chem* 2004;**279**:52630–52642.
14. Shizukuda Y, Matoba S, Mian OY, Nguyen T, Hwang PM. Targeted disruption of p53 attenuates doxorubicin-induced cardiac toxicity in mice. *Mol Cell Biochem* 2005;**273**: 25–32.
15. Tachibana H, Naga Prasad SV, Lefkowitz RJ, Koch WJ, Rockman HA. Level of beta-adrenergic receptor kinase 1 inhibition determines degree of cardiac dysfunction after chronic pressure overload-induced heart failure. *Circulation* 2005;**111**:591–597.
16. Komarova EA, Chernov MV, Franks R, Wang K, Armin G, Zelnick CR *et al*. Transgenic mice with p53-responsive lacZ: p53 activity varies dramatically during normal development and determines radiation and drug sensitivity *in vivo*. *EMBO J* 1997;**16**: 1391–1400.
17. Gupta S, Sen S. Role of the NF-kappaB signaling cascade and NF-kappaB-targeted genes in failing human hearts. *J Mol Med* 2005;**83**:993–1004.
18. Ju J, Schmitz JC, Song B, Kudo K, Chu E. Regulation of p53 expression in response to 5-fluorouracil in human cancer RKO cells. *Clin Cancer Res* 2007;**13**:4245–4251.
19. Rouet-Benzineb P, Gontero B, Dreyfus P, Lafuma C. Angiotensin II induces nuclear factor-kappa B activation in cultured neonatal rat cardiomyocytes through protein kinase C signaling pathway. *J Mol Cell Cardiol* 2000;**32**:1767–1778.
20. Onohara N, Nishida M, Inoue R, Kobayashi H, Sumimoto H, Sato Y *et al*. TRPC3 and TRPC6 are essential for angiotensin II-induced cardiac hypertrophy. *EMBO J* 2006;**25**: 5305–5316.
21. Peng Y, Popovic ZB, Sopko N, Drinko J, Zhang Z, Thomas JD *et al*. Speckle tracking echocardiography in the assessment of mouse models of cardiac dysfunction. *Am J Physiol Heart Circ Physiol* 2009;**297**:H811–H820.
22. Naga Prasad SV, Duan ZH, Gupta MK, Surampudi VS, Volinia S, Calin GA *et al*. A unique microRNA profile in end-stage heart failure indicates alterations in specific cardiovascular signaling networks. *J Biol Chem* 2009;**284**:27487–27499.
23. Dignam JD, Martin PL, Shastry BS, Roeder RG. Eukaryotic gene transcription with purified components. *Methods Enzymol* 1983;**101**:582–598.
24. Gupta S, Purcell NH, Lin A, Sen S. Activation of nuclear factor-kappaB is necessary for myotrophin-induced cardiac hypertrophy. *J Cell Biol* 2002;**159**:1019–1028.
25. Venkatachalam S, Shi YP, Jones SN, Vogel H, Bradley A, Pinkel D *et al*. Retention of wild-type p53 in tumors from p53 heterozygous mice: reduction of p53 dosage can promote cancer formation. *EMBO J* 1998;**17**:4657–4667.
26. Sil P, Misono K, Sen S. Myotrophin in human cardiomyopathic heart. *Circ Res* 1993;**73**: 98–108.
27. Sil P, Gupta S, Young D, Sen S. Regulation of myotrophin gene by pressure overload and stretch. *Mol Cell Biochem* 2004;**262**:79–89.
28. Sil P, Mukherjee DP, Sen S. Quantification of myotrophin from spontaneously hypertensive and normal rat hearts. *Circ Res* 1995;**76**:1020–1027.
29. O'Brien RJ, Loke I, Davies JE, Squire IB, Ng LL. Myotrophin in human heart failure. *J Am Coll Cardiol* 2003;**42**:719–725.
30. Song H, Conte JV Jr, Foster AH, McLaughlin JS, Wei C. Increased p53 protein expression in human failing myocardium. *J Heart Lung Transplant* 1999;**18**:744–749.
31. Li P, Li J, Feng X, Li Z, Hou R, Han C *et al*. Gene expression profile of cardiomyocytes in hypertrophic heart induced by continuous norepinephrine infusion in the rats. *Cell Mol Life Sci* 2003;**60**:2200–2209.
32. Matsusaka H, Ide T, Matsushima S, Ikeuchi M, Kubota T, Sunagawa K *et al*. Targeted deletion of p53 prevents cardiac rupture after myocardial infarction in mice. *Cardiovasc Res* 2006;**70**:457–465.
33. Depke M, Steil L, Domanska G, Volker U, Schutt C, Kiank C. Altered hepatic mRNA expression of immune response and apoptosis-associated genes after acute and chronic psychological stress in mice. *Mol Immunol* 2009;**46**:3018–3028.
34. Cao X, Plasencia C, Kanzaki A, Yang A, Burke TR Jr, Neamati N. Elucidation of the molecular mechanisms of a salicylhydrazide class of compounds by proteomic analysis. *Curr Cancer Drug Targets* 2009;**9**:189–201.
35. McCarthy N, Mercer J, Bennett M. Apoptotic proteins. p53 and c-myc related pathways. *Cardiol Clin* 2001;**19**:75–89. viii.
36. Olivetti G, Abbi R, Quaini F, Kajstura J, Cheng W, Nitahara JA *et al*. Apoptosis in the failing human heart. *N Engl J Med* 1997;**336**:1131–1141.
37. Moorjani N, Catarino P, Trabzuni D, Saleh S, Moorji A, Dzimiri N *et al*. Upregulation of Bcl-2 proteins during the transition to pressure overload-induced heart failure. *Int J Cardiol* 2007;**116**:27–33.
38. Gupta S, Young D, Maitra RK, Gupta A, Popovic ZB, Yong SL *et al*. Prevention of cardiac hypertrophy and heart failure by silencing of NF-kappaB. *J Mol Biol* 2008; **375**:637–649.
39. Dreyfus DH, Nagasawa M, Gelfand EW, Ghoda LY. Modulation of p53 activity by IkappaBalpha: evidence suggesting a common phylogeny between NF-kappaB and p53 transcription factors. *BMC Immunol* 2005;**6**:12.
40. Webster GA, Perkins ND. Transcriptional cross talk between NF-kappaB and p53. *Mol Cell Biol* 1999;**19**:3485–3495.
41. Beg AA, Baltimore D. An essential role for NF-kappaB in preventing TNF-alpha-induced cell death. *Science* 1996;**274**:782–784.
42. Bertrand F, Atfi A, Cadoret A, L'Allemain G, Robin H, Lascols O *et al*. A role for nuclear factor kappaB in the antiapoptotic function of insulin. *J Biol Chem* 1998;**273**: 2931–2938.
43. Klefstrom J, Arighi E, Littlewood T, Jaattela M, Saksela E, Evan GI *et al*. Induction of TNF-sensitive cellular phenotype by c-Myc involves p53 and impaired NF-kappaB activation. *EMBO J* 1997;**16**:7382–7392.
44. Hall PA, Meek D, Lane DP. p53—integrating the complexity. *J Pathol* 1996;**180**:1–5.
45. Levine AJ. p53, the cellular gatekeeper for growth and division. *Cell* 1997;**88**:323–331.